

1 **Supplementary information**

2 **Use of spatiotemporal characteristics of ambient PM_{2.5} in rural South India to infer**

3 **local versus regional contributions**

4 M. Kishore Kumar, V. Sreekanth, Maëlle Salmon, Cathryn Tonne,

5 Julian D. Marshall

6

7 Contents

8 **SI.1 methods**

9 SI. 1.1 Alternate under-writing function

10 SI. 1.2 Estimation of atmospheric transport and diffusion

11 **SI. 2 Results**

12 Figure SI. 2.1. Real time RH correction

13 Figure SI. 2.2. eBAM-DustTrak collocation

14 Figure SI. 2.3. Distributions of PM_{2.5} concentrations measured at three ambient sites

15 Figure SI. 2.4. Week wise PM_{2.5} at the three rural sites

16 Figure SI. 2.5. Data Availability

17 Figure SI. 2.6. Season wise PM_{2.5} variations at the three sites based on common days data

18 Figure SI. 2.7. Box plots of skew variations at three rural sites

19 Figure SI. 2.8. Season wise urban-rural PM_{2.5} variations

20 Figure SI. 2.9. Local and regional scale contributions using alternate underwriting function

21 Figure SI. 2.10. Locations of brick kilns and rice mills around three rural sites

22 Figure SI. 2.11. Season wise wind roses for North site

23 Figure SI. 2.12. Season wise wind roses for Central site

24 Figure SI. 2.13. Season wise wind roses for South site

25 Table SI. 2.1. PM_{2.5} concentrations during weekdays and weekends

26 Table SI. 2.2. Season wise ratios of PM_{2.5} levels at the three ambient sites

27 Table SI. 2.3. Local source contributions based on moving average subtraction method

28 Table SI. 2.4. Local source contributions based on alternate underwriting function

29 Table SI. 2.5. Percentage of days with stagnation, recirculation, ventilation, and stagnation-

30 recirculation events

31 Table SI. 2.6. Percentage of stagnation, recirculation and ventilation events during various

32 seasons

33 Table SI. 2.7. Hourly median PM_{2.5} concentrations ($\mu\text{g m}^{-3}$) during various wind speeds.

34 Table SI. 2.8. Hourly median PM_{2.5} concentrations ($\mu\text{g m}^{-3}$) during various wind directions

35 Table SI. 2.9. Average and standard deviations of monthly temperature and relative humidity

36 (RH) over the study area

37

38

39

40 **SI.1 methods**

41 **SI. 1.1 Alternate under-writing function**

42 We used an alternate under writing function to validate the results from the moving average
43 subtraction method. In the past, few studies reported that the moving average subtraction
44 method often underestimates the proportion of concentrations attributable to local emissions
45 and over estimates the strength of regional sources (Both et al., 2011). In the present study,
46 we employed an alternative underwriting function that selects, for each time point, the second
47 lowest value from a 360 min moving window.

48 **SI. 1.2 Estimation of atmospheric transport and diffusion**

49 We estimated atmospheric conditions by means of stagnation, ventilation, and recirculation
50 analysis proposed by Allwine and Whiteman (1994). During stagnation,winds are slow or
51 stagnant altogether, resulting in accumulation of pollutants in the vicinity of a source. During
52 recirculation,pollutants are initially transported from source but later return; this pattern
53 mayresult a pollution episode. During ventilation,polluted air is carried away by fresh air.

54 We calculated the representative integral quantities for stagnation and recirculation using
55 measured wind speed (U_i) and direction (D_i). For a given wind speed and direction, the wind
56 components were expressed as follows:

57
$$n_i = U_i \cos(D_i - 180) \quad (1)$$

58
$$e_i = U_i \sin(D_i - 180) \quad (2)$$

59 Where $i=1, \dots, N$, n_i and e_i represent North-South and east-west component respectively for
60 each discrete data point i .

61 The North-South transport distance (X_i) and east-west transport distance (Y_i) for an averaging
62 time interval T were estimated using equation (3) and (4), respectively.

63
$$X_i = T \sum_{j=i}^{i+p} n_j \quad (3)$$

64
$$Y_i = T \sum_{j=i}^{i+p} e_j \quad (4)$$

65 where, $i=1, \dots, N-p$; $p = \tau/T - 1$; $\tau =$ Transport time.

66 The resultant transport distance (L_i) was computed as

67
$$L_i = \sqrt{X_i^2 + Y_i^2} \quad (5)$$

68 The wind run (S_i) and recirculation factor (R_i) were computed as

69
$$S_i = T \sum_{j=i}^{i+p} U_j \quad (6)$$

70
$$R_i = 1 - \frac{L_i}{S_i} \quad (7)$$

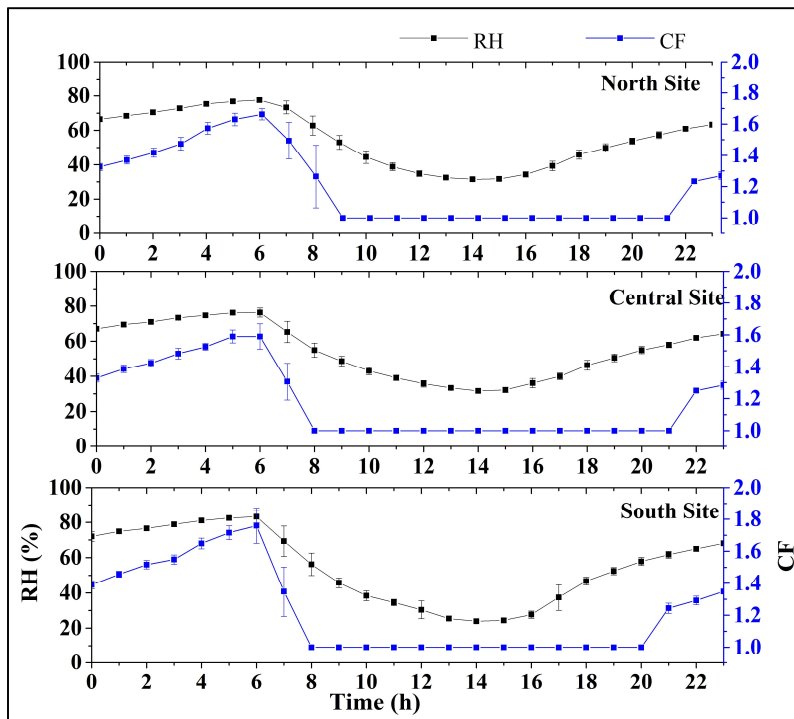
71
72 If $S_i \leq S_c$, asite is prone to stagnation.

73 If $R_i \geq R_c$, asite is prone to recirculation.

74 If $R_i \leq R_{cv}$ and $S_i \geq S_{cv}$, a site is prone to ventilation.

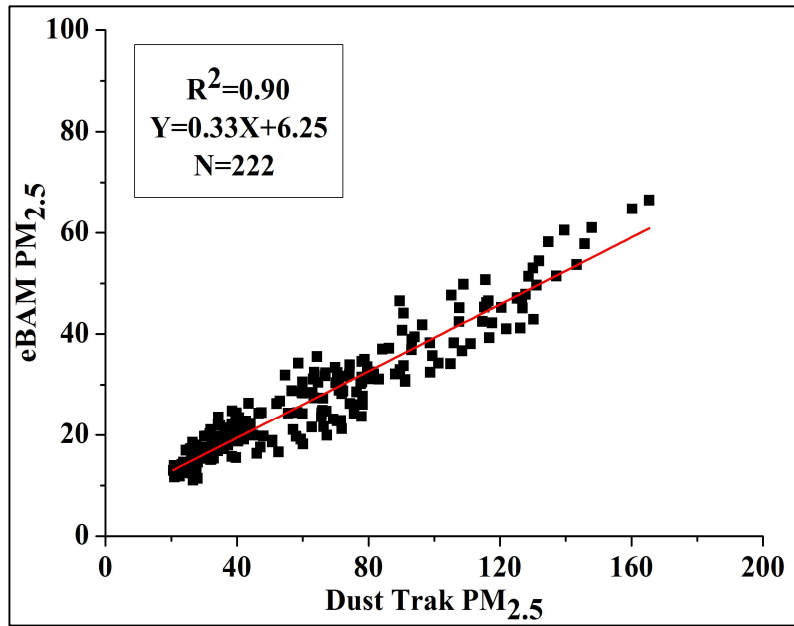
75 Here, S_c and R_c are average daily critical transport indices (CTIs) for stagnation and
76 recirculation, respectively. The CTI parameters are estimated as the average wind run and
77 average recirculation factor during the monitoring period, respectively. S_{cv} and R_{cv} are the
78 CTIs for ventilation and are computed as 75th percentile of S_i and 25th percentile of R_i ,
79 respectively (Chithra et al., 2014). The transport labels (“stagnation” and “recirculation”) are
80 not mutually exclusive, that is, a day might receive more than one label.

81



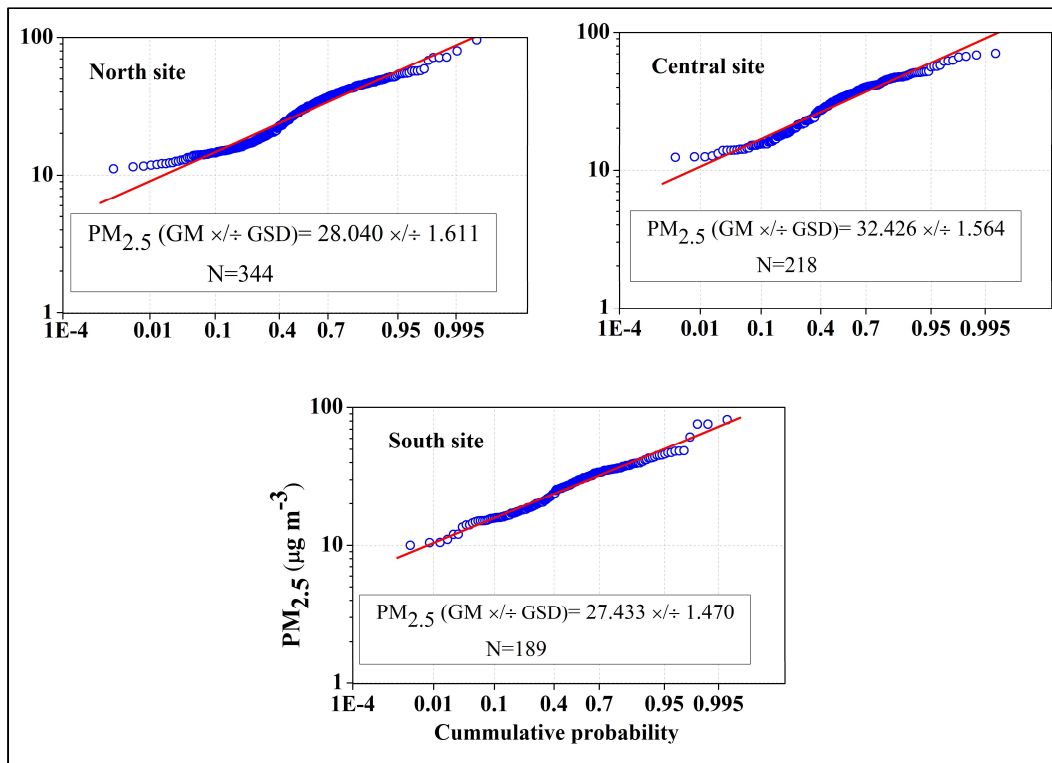
82
83
84
85
86

Figure SI.2.1. Median relative humidity (RH) and nephelometer correction factor by time of day and site (see equations 1 and 2 in main text). Error bars represent interquartile ranges (IQR).



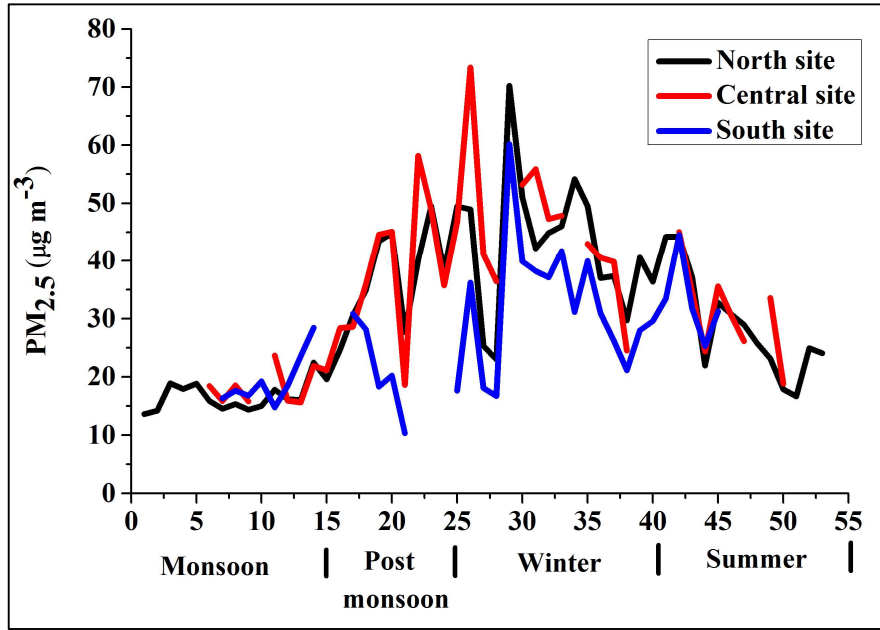
87
88
89
90
91

FigureSI.2.2. Comparison between 24h average $PM_{2.5}$ concentrations for collocated eBAM and RH-corrected DustTrak measurements. The best-fit line is the correction factor applied to all DustTrak measurements presented in this study.



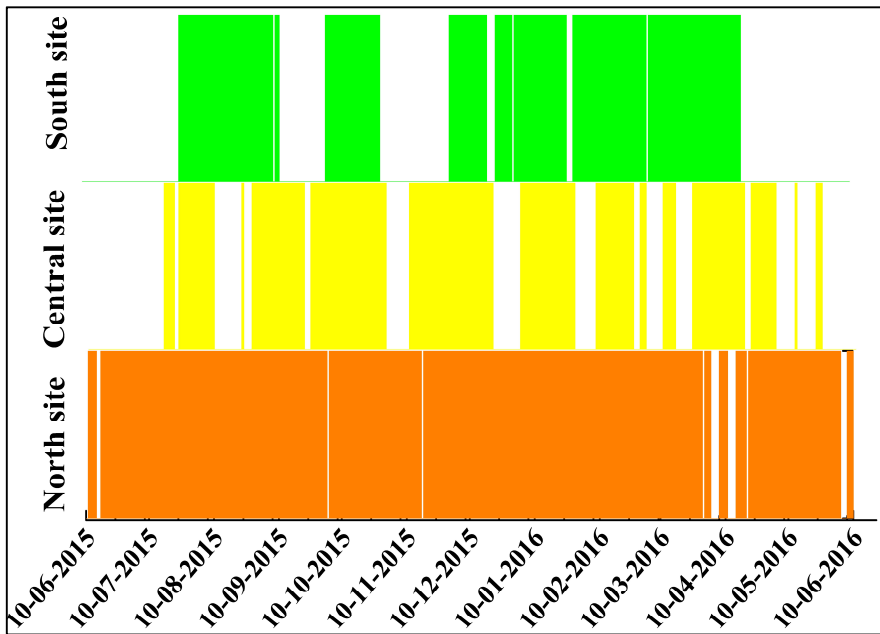
92
93
94
95
96
97

Figure SI.2.3. Lognormal probability plots for 24 h averaged $PM_{2.5}$ concentrations measured at north, central and south sites. The lines within figures indicate best-fit lognormal distributions. Text boxes report geometric mean \times/\div geometric standard deviation; N represents the number of valid samples for each site.



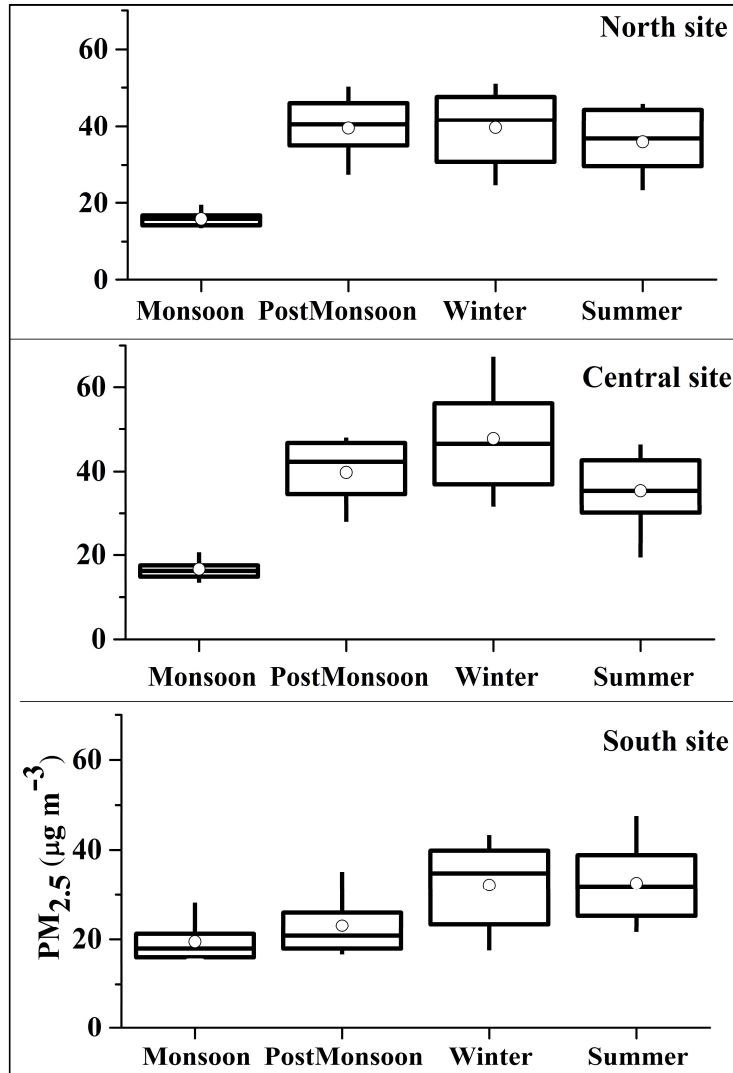
98
99
100
101

Figure SI. 2.4. Weekly average PM_{2.5} concentrations at the three rural ambient sites. Here, week 1 starts 11 June 2016.



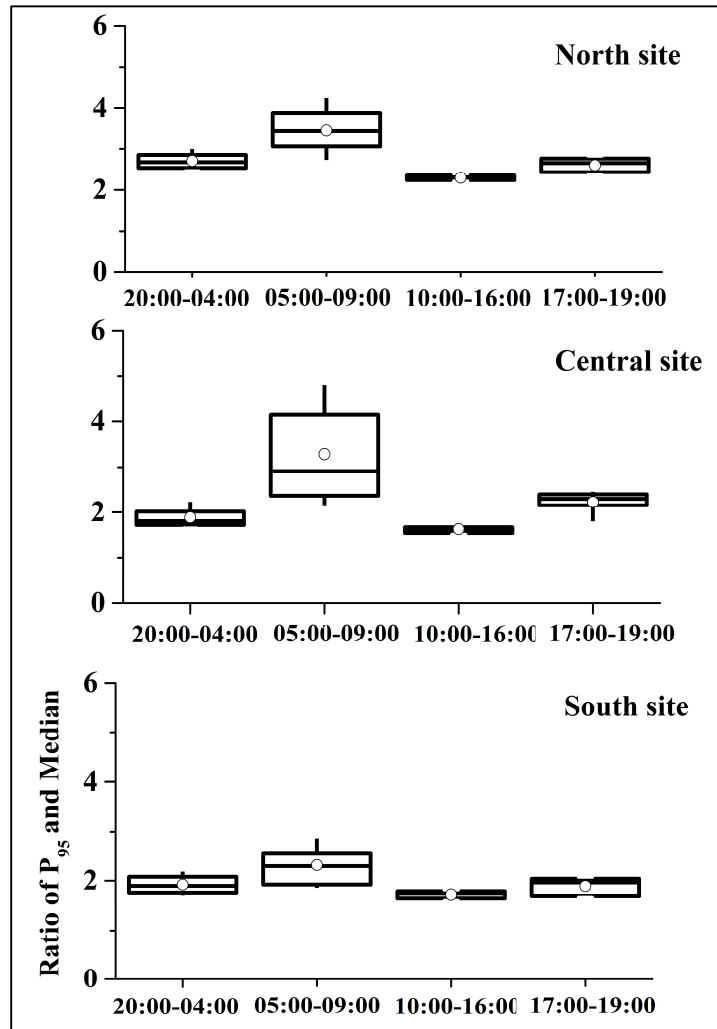
102
103
104
105
106
107
108
109
110
111
112

Figure SI.2.5. PM_{2.5} data collection over time (DustTrak and eBAM data) according to site. Gaps represent missing data (e.g., instrument malfunction, power outage). Total data collection: 344 days North site; 218 days Central site; 189 days South site.



114
 115
 116
 117
 118

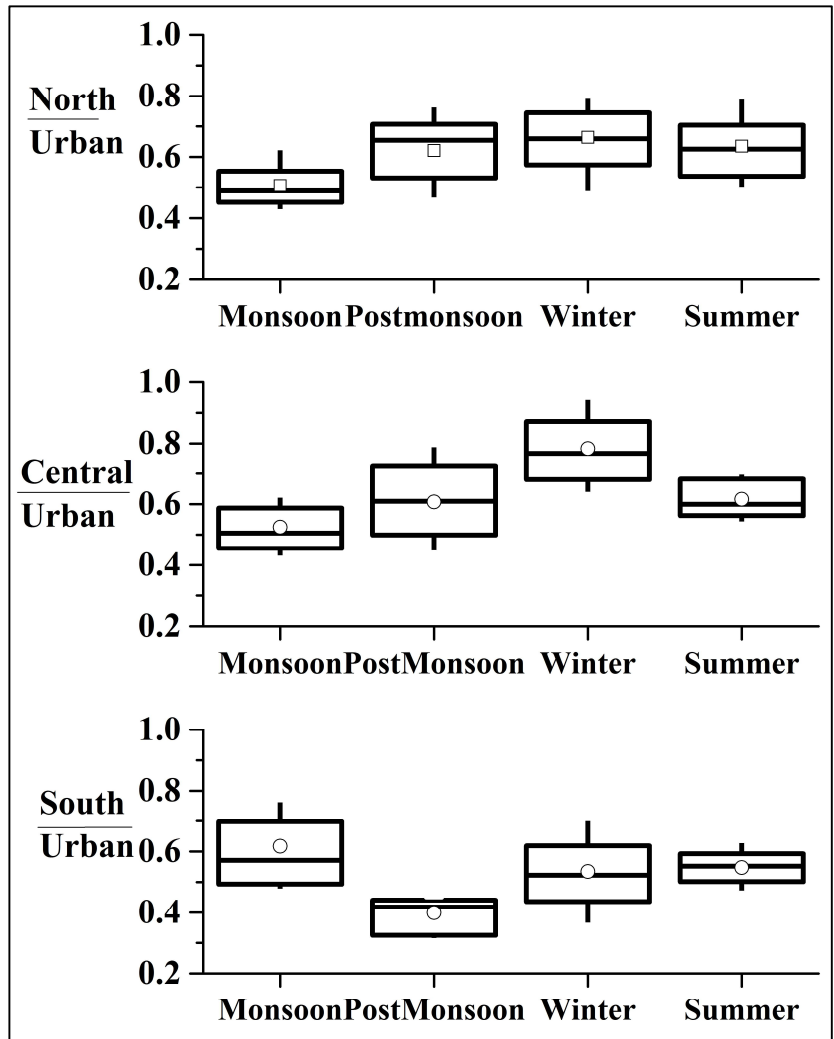
Figure SI.2.6. Variability of 24h averaged $PM_{2.5}$ concentrations according to site and season based on 139 days common data.



119

120 **Figure SI. 2.7.** Box plots of PM_{2.5} concentrations sampled at the three ambient sites showing
 121 a measure of skew (ratio of minute 95th percentile [P95] to 24h median concentration based
 122 on 1 min medians of concentration)

123



124

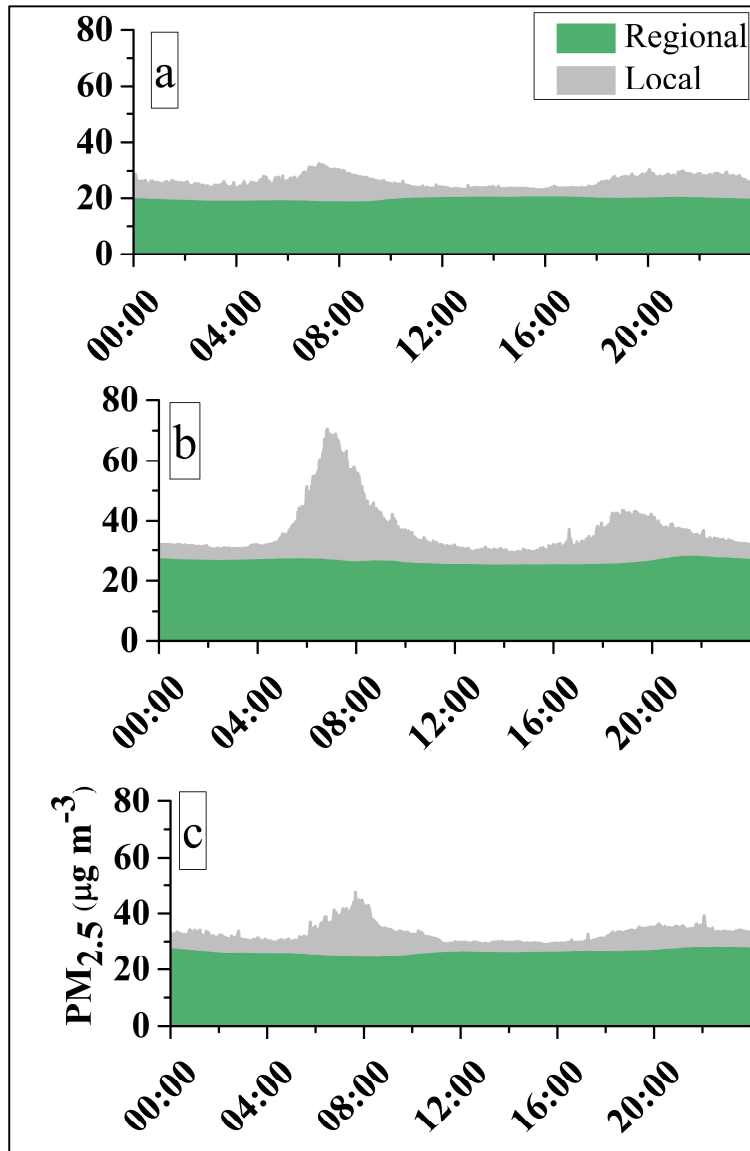
125

126

127

128

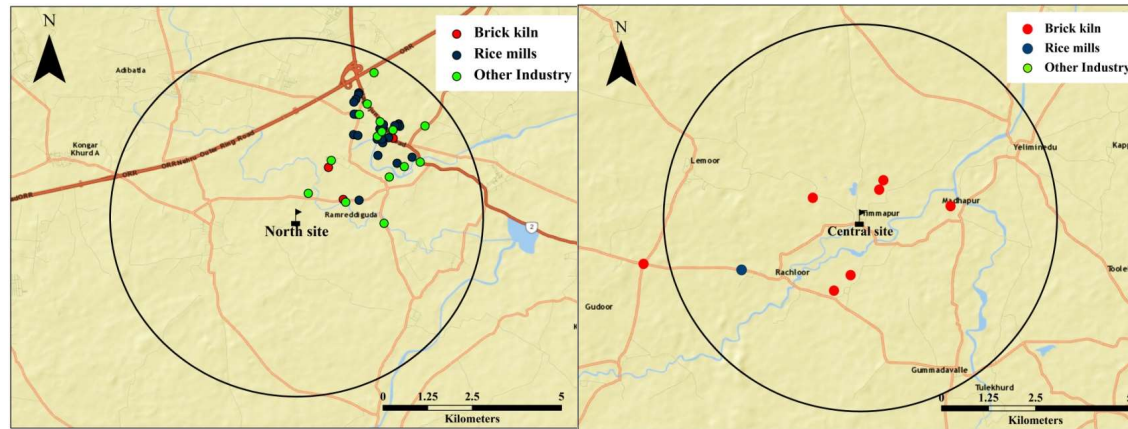
Figure SI.2.8. Season wise distribution of rural-urban PM_{2.5} ratios for three rural sites



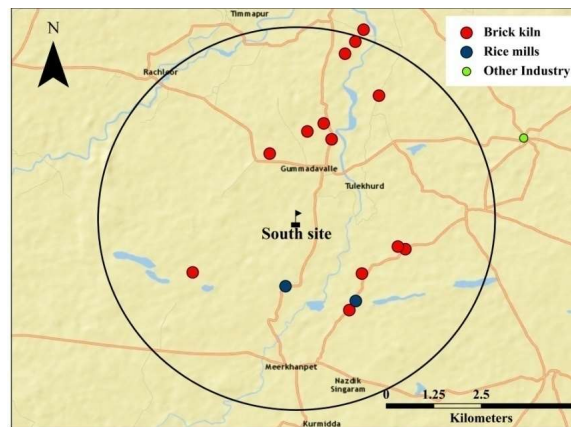
129
 130
 131
 132
 133
 134

Figure SI.2.9. Median PM_{2.5} concentration by local and regional scale contributions, by time of day at (a) North site (b) Central site and (c) South site location using alternate underwriting function

135



136

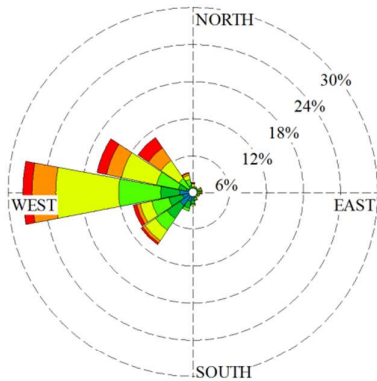


137

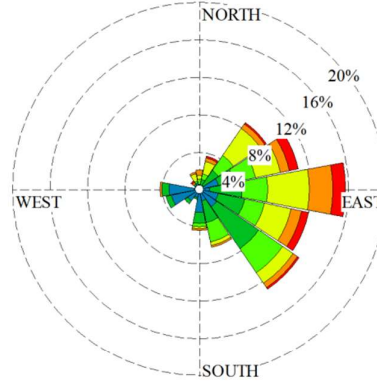
138

Figure SI.2.10. Aerial view of brick kilns, rice mills and other industries present in 5 km radius around three rural sites.

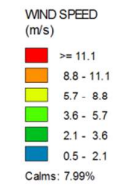
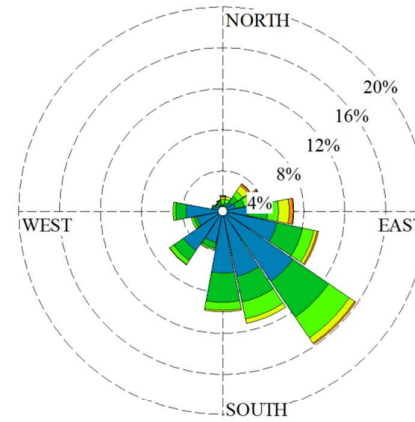
a



b

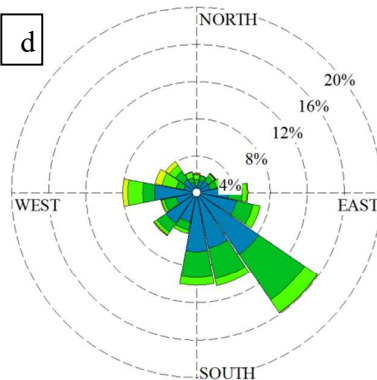


c

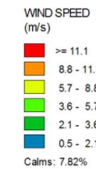
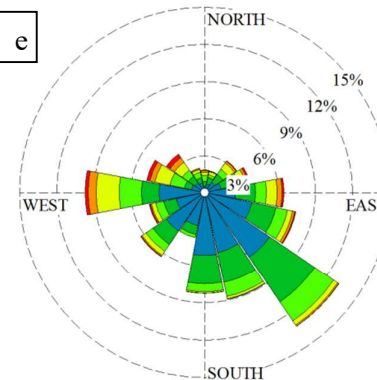


139

d

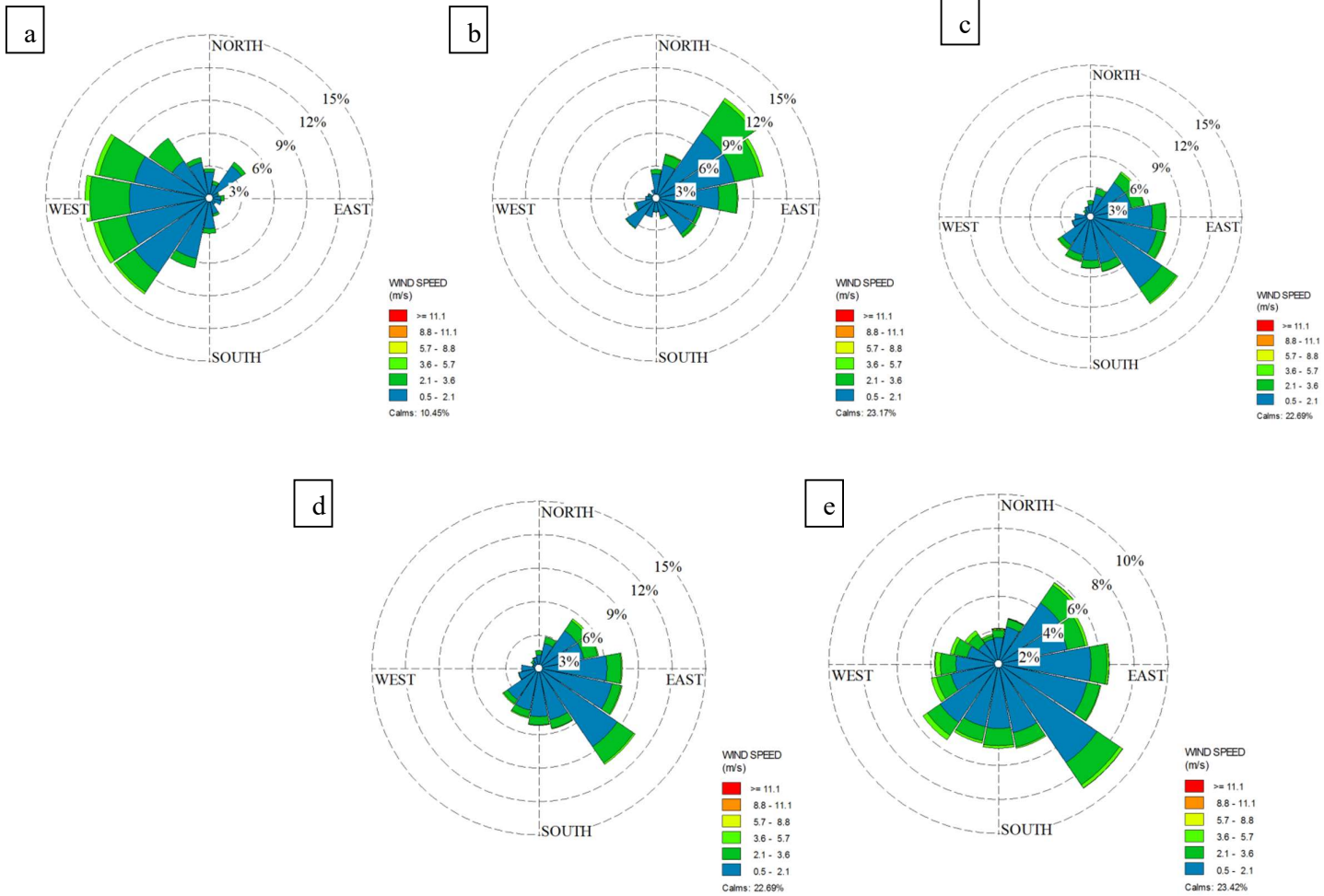


e



140

Figure SI.2.11. Wind roses showing wind speed and direction for the (a) monsoon, (b) post monsoon, (c) winter, (d) summer and (e) total monitoring period at the North site. Here and elsewhere, wind rose represent the direction from which wind blows



141

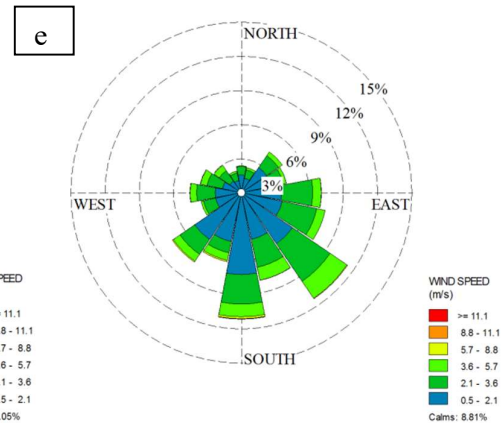
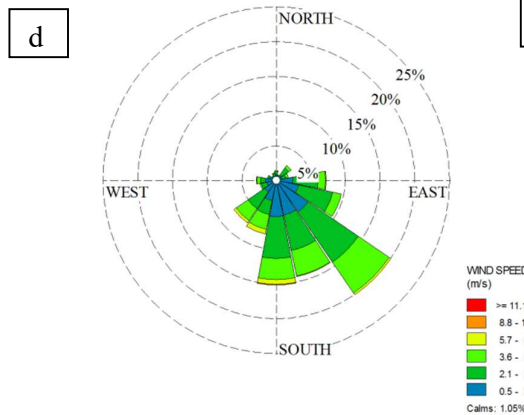
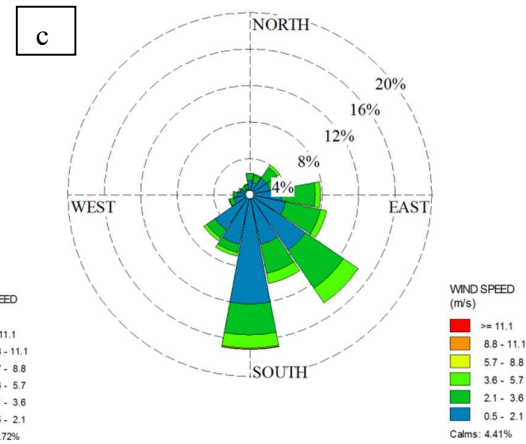
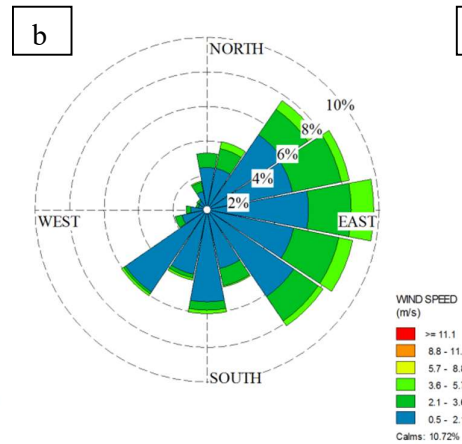
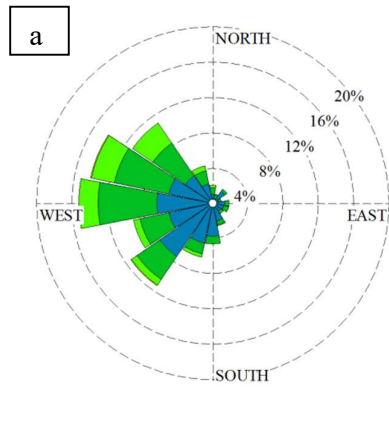
142

143

144

145

Figure SI.2.12. Wind roses showing wind speed and direction for the (a) monsoon, (b) post monsoon, (c) winter, (d) summer and (e) total monitoring period at Central site.



146

147

148

149

150

Figure SI.2.13. Wind roses showing wind speed and direction for the (a) monsoon, (b) post monsoon, (c) winter, (d) summer and (e) total monitoring period at South site

151

152

Table SI.2.1. PM_{2.5} concentrations (µgm⁻³) during weekdays and weekends

	North site	Central site	South site
WeekendMedian (P25, P75)	29 (18,41)	35 (22,45)	29 (19,37)
WeekdayMedian (P25, P75)	29 (19,42)	37 (23,48)	30 (21,36)
Weekend (24 hr GM ×/÷GSD)	28.723×/÷ 1.626	32.370×/÷1.576	28.506×/÷1.481
Weekday (24 hr GM ×/÷GSD)	27.768×/÷1.606	32.450×/÷1.561	27.036×/÷1.467
All daysMedian (P25, P75)	29 (18,41)	35 (23,46)	29 (20,37)
All days (24 hr GM ×/÷GSD)	28.040×/÷1.611	32.426×/÷1.564	27.433×/÷1.470

153

154

155

156

157

158

Table SI.2.2 Season wise ratios of medians of 24h averaged PM_{2.5} levels at the three ambient sites

Ratios	Central North	Central South	North South
Monsoon	1.03	0.92	0.84
Post-Monsoon	1.01	2.21	2.1
Winter	1.19	1.47	1.21
Summer	0.99	1.08	1.13
All days	1.06	1.23	1.15

159

160

161

162

163

164

Table SI. 2.3.Percentage of local concentrations computed based on moving average subtraction method at the different time intervals of a day.

Site	Averagecontributions at different time scales					
	(00:00-23:00)	(00:00-05:00)	(05:00-09:00)	(09:00-17:00)	(17:00-20:00)	(20:00-23:00)
North	11	12	17	6	9	14
Centra l	12	6	25	8	17	9
South	8	7	16	5	7	7

165

166

167

168

169 **Table SI.2.4.** Percentage of local concentrations computed based on alternate underwriting
 170 function at the different time intervals of a day

Site	Average contributions at different time scales					
	(00:00-23:00)	(00:00-04:00)	(05:00-08:00)	(09:00-16:00)	(17:00-19:00)	(20:00-23:00)
North	25	25	35	17	24	30
Central	26	15	47	21	34	23
South	20	18	33	16	20	21

171

172

173

174

175

176 **Table SI. 2.5.**Percentage of days with stagnation, recirculation, ventilation, and stagnation-
 177 recirculation events at three rural sites

Site	Percentage of stagnation days	Percentage of recirculation days	Percentage of Ventilation days	Percentage of days with both stagnation and recirculation events
North site	64	44	16	29
Central site	63	41	8	34
South site	61	49	6	29

178

179

180

181

182 **Table SI. 2.6.**Percentage of stagnation, recirculation and ventilation events during monsoon,
 183 post monsoon, winter and summer events at three rural sites.

Site	Event	Monsoon	Post Monsoon	Winter	Summer	Annual
North site	Stagnation	2	2	55	41	64
	Recirculation	15	6	42	36	44
	Ventilation	51	15	22	12	16
Central site	Stagnation	10	39	39	12	63
	Recirculation	14	26	28	32	41
	Ventilation	55	5	20	20	8
South site	Stagnation	18	44	35	3	61
	Recirculation	14	33	36	18	49
	Ventilation	50	7	14	29	6

184

185

186

187 **Table SI. 2.7.**Hourly median PM_{2.5} concentrations (µg m⁻³) during wind speeds. The number
 188 of hours of PM_{2.5} episode occurrences is within brackets

Wind speed (m/sec)	North site	Central site	South site
≤0.5 (calm conditions)	47 (156)	43(355)	34 (55)
0.6-2	38 (222)	34(104)	31 (73)
2-4	29 (83)	30(17)	29 (28)
≥4	22(49)	23(0)	29 (4)

189

190

191

192

193 **Table SI.2.8.** Hourly median PM_{2.5} concentrations (µg m⁻³) during various wind direction
 194 periods at the three rural sites

Wind direction	North site	Central site	South site
0≤θ<45	32	41	37
45≤θ<90	37	40	34
90≤θ<135	35	38	31
135≤θ<180	34	36	30
180≤θ<225	32	40	31
225≤θ<270	30	37	29
270≤θ<315	29	36	27
315≤θ<360	27	40	31

195

196 **Table SI.2.9.**Average and standard deviations of monthly temperature and relative humidity
 197 (RH) over the study area

	Temp (°C)		RH (%)	
	Average	SD	Average	SD
Jan	24.02	6.34	49.71	21.79
Feb	27.83	6.4	44.71	22.12
Mar	30.85	6.58	39.55	22.69
Apr	33.66	6.53	33.42	21.86
May	33.19	5.34	42.68	16.65
Jun	30.54	5.19	53.89	16.92
Jul	29.68	4.41	55.37	15.43
Aug	27.49	4.15	68.13	16.08
Sep	27.28	4.87	71.34	18.24
Oct	27.19	5.45	63.46	20.91
Nov	24.8	4.93	61.75	19.4
Dec	24.32	5.99	55.16	21.71

198

199